ABSTRACT

DROWSY DRIVER DATA AQCUISITION SYSTEM

By Rafael Norat

This thesis focuses on detecting the drowsiness of a driver based on differentiation of the EEG signal activity between the eyes open and eyes closed states. Here, it is observed that there is a significant increase in a 10 Hz component of the alpha rhythm activity when the subject under test closes his / her eyes. This phenomenon was observed when electrodes were attached to the occipital region. A more desirable approach is to develop a non-intrusive measurement based on a multi-turn differential coil combination utilizing a low noise high gain amplifier. The system developed here used an 80,000 turn 2 coil differential combination. A 10 Hz band pass amplifier with a gain of 68 db confirmed the assumed changes when electrodes were used. However, when differential coils were used (80,000 differential coils), the system failed to validate the expected changes. Due to insufficient sensitivity, it was impossible to reach a conclusion and determine whether the increased 10 Hz activity corresponded to brain signals or increased feedback gain resulting in an internal oscillation within the high gain amplification of the developed system. Further studies are suggested to reduce the losses due to magnetic core material and design an amplifier with a lower noise figure. The system developed utilized a DaqCard-1200 data acquisition card and MATLAB for signal processing.

DROWSY DRIVER DATA ACQUISITION SYSTEM

by
Rafael Norat

A Thesis
Submitted to the Faculty of
New Jersey Institute of Technology
In Partial Fulfillment of the Requirements for the Degree of
Master of Science in Biomedical Engineering

Biomedical Engineering Committee

August 2000

APPROVAL PAGE

DROWSY DRIVER DATA ACQUISITION SYSTEM

Rafael Norat

Dr. Edip Niver, Thesis Adviser   **Date**
Associate Professor of Electrical Engineering, NJIT

Dr. John Tavantzis   **Date**
Professor of Mathematics

Dr. Ibrahim Akduman   **Date**
Dean of Electrical and Electronics Engineering, Istanbul Technical University

---

Dr. Kyriacos Mouskos   **Date**
Assistant Professor of Civil Engineering, NJIT

Dr. Raashid Malik   **Date**
Visiting Professor of Electrical and Computer Engineering, NJIT

BIOGRAPHICAL SKETCH

Author: Rafael Norat

Degree: Master of Science in Biomedical Engineering

Date: July 2000

Undergraduate and Graduate Education:

- Master of Science in Biomedical Engineering
  New Jersey Institute of Technology, Newark, NJ, 2000

- Bachelor of Science in Electrical Engineering
  New Jersey Institute of Technology, Newark, NJ, 1997

Major: Biomedical Engineering

This thesis is dedicated to my family for having faith in me.

ACKNOWLEDGEMENT

The author wishes to express his sincere gratitude to Dr. Niver, for his guidance and patience through the entire process. Without his support, insight, and intuition, none of this would have been possible.

Special thanks are extended to all the graduate students who are working along with Dr. Niver, for all their help and support.

TABLE OF CONTENTS

Chapter	Page

TABLE OF CONTENTS
(Continued)

LIST OF FIGURES

Figure   **Page**

LIST OF FIGURES
(continued)

Figure   **Page**

CHAPTER 1

INTRODUCTION

Over the years, drowsy driving has continuously been a problem, especially with it's inherent difficulties in monitoring and deterring. The National Highway Traffic Safety Administration (NHTSA) estimates that each year, approximately 1,550 people are killed and 40,000 people are injured in crashes related to, if not primarily caused by, drowsy driving [1]. Accident reports on drowsy driving convey only partial incidents, as many accidents are left unreported and are attributed to a cause other than drowsy driving. It is often a difficult task for a person to observe his own state of awareness while driving, which can lead to a last minute life-threatening decision. A 1994 survey conducted by the Institute for Traffic Safety and Fact Finders, Inc. found that about half of the New York State drivers polled reported drowsy while driving within the previous year and 25 percent of the driver reported having fallen asleep at the wheel [2]. Also in 1994, approximately 9 percent of wheeled vehicle driving accidents resulting in injury or death during Operation Desert Shield and Desert Storm was attributed to driver drowsiness/fatigue [3].

With these conditions in mind, the NHTSA as well as other traffic safety organizations have focussed their attention on determining, analyzing, and correcting the problems of driver drowsiness. Educational campaigns have been launched in order to alert individuals of the dangers behind drowsy driving. Young males between the ages of 16 and 24 as well as shift workers have been specifically targeted by these campaigns. Road warnings such as shoulder rumple strips have been created as a countermeasure towards drowsy driving [4].

Recording methods have been developed in order to provide a better insight on detecting the initial stages of drowsy driving. Simulation chambers such as the National Advanced Driving Simulator (NADS) can now offer real-time analysis of driver and vehicle responses to just about any highway driving scenario without putting the subjects at risk. Recording and analysis devices such as the Portable Driver Performance Data Acquisition System for Crash Avoidance Research (DASCAR) utilize sensors and video cameras to provide real-world in-vehicle data while remaining unobtrusive to the subjects, in effect providing a "naturalistic" study [5]. These instruments are in the constant process of improvements in order to some day provide a universal drowsiness alarm system.

1.1 Drowsy-Driver Analysis

Loss of Alertness (LOA) describes a mental state during which the operator's internal response to external stimuli is insufficient. "Drowsiness" is a term used in NHTSA studies to refer to a state of reduced alertness, usually accompanied by decreased performance and physiological changes that may result in loss of alertness or being asleep at the wheel. Monitoring drowsiness therefore takes on the responsibility of recording the performance and physiological changes associated with drowsiness [6].

Performance changes can be monitored through the use of video cameras and sensors, which detect changes in vehicle and human response. Vehicle sensors can use criteria such as steering angle and brake pedal acceleration to determine states of alertness. Performance measurements such as "drift and jerk" steering and delayed or excessive braking have been used in various studies to determine states of alertness.

Visual measurements employ the individual's sensory input in determining the state of alertness by observing one's head/eye movement, glance frequency, or glance duration through a video camera [7]. Through its use in various drowsiness studies conducted by the NHTSA, eye closure has proven to be a reliable gauge in determining drowsiness states of driving. PERCLOS, defined as the proportion of a time interval that the eyes were 80% to 100% closed (exclusive of blinks), has been proven to correlate with other physiological indicators of drowsiness, such as electroencephalogram (EEG) and electrocardiogram (EKG) records [8]. Studies such as the "Three-in-one Vehicle Operator Sensor" conducted by the Northrop Grumman Corporation employed PERCLOS as their primary indicator of drowsiness through the use of video recording [9].

Physiological changes can be monitored through a wide variety of measurements, which include EKG, EEG, electromyogram (EMG), galvanic skin resistance (GSR), respiration rate, body temperature, as well as others [10]. All methods are valid and reliable indicators of drowsiness. However, minor-to-moderate obtrusiveness to the driver still remains an issue. This thesis focuses on the usage of EEG in early detection of drowsiness. Variations in the EEG signals have much faster response time in detecting drowsiness when compared to other physiological indicators. It is imperative to concentrate on the method which would have the capability of immediately detecting drowsy behavior because a split second delay may result in fatal accidents.

CHAPTER 2

THE ELECTROENCEPHALOGRAM (EEG)

The electric potential fluctuations recorded from the brain by Hans Berger in the nineteenth century form the basis for modern electroencephalography (EEG). Previous studies had recorded background electrical activity of the brain in unanesthetized animals, but it was Hans Berger's systematic research which lead to the evolution of the electroencephalogram as a modern clinical tool, and became an indispensable instrument for brain wave analysis [11]. It serves well in diagnosing certain brain and nervous system conditions such as epilepsy, mental confusion, and sleep disorders. By analyzing the patient's brain activity during resting as well as during reactionary states, the EEG can lead to characterize the state of the mental health of an individual.

2.1 Electrodes and EEG Recording

Electrical activity of the brain is recorded with three types of electrodes: scalp, cortical, and depth electrodes. Recordings with electrode placement on the cortex of the brain are termed electrocorticogram (EcoG). Depth recording is performed through the placement of electrodes into the neural tissue of the brain. Scalp recording is achieved by attaching an electrode to the scalp through a conducting medium. These electrodes serve as the transducing interface between the ionic current of the body and the electron current of the instrumentation.

EEG recordings are obtained through the use of a differential amplifier following three different types of electrode connections:

- between each member of a pair or "bipolar",

- between one monopolar lead and a distant reference electrode, and

4

- between one monopolar lead and the average of all.

In a bipolar system, differential measurements are made between successive pairs of electrodes. The electric potential changes are then amplified by high-gain, low-noise differential amplifiers. Output signals are then displayed digitally or through ink-writing strip chart recorders and often are stored in computers using data acquisition cards.

EEG recordings are routinely obtained with the subject in resting state with eyes closed. The subject must remain in a still, relaxed position in order to eliminate any possible artifact such as electrode-lead movement or muscle artifact, which is perhaps the most common type of interference. Facial muscles can produce signals well within the EEG range (0.5-100 Hz), and must therefore be distinguished from brain activity.

2.2 The Cerebrum

The architecture of the neuronal brain tissue is not uniform. Therefore, EEG recordings will vary in information from one recording location to another. The measuring platform for the EEG is the cerebrum, which is part of our central nervous system. The cerebrum is a paired structure, with right and left hemispheres that control the reaction to the opposite side's stimulus. Each hemisphere consists of several layers, with the outer most being the cerebral cortex. The cerebral cortex is further divided into 4 lobes: frontal, parietal, temporal, and occipital. Each lobe conveys different information based on sensory responses to stimulus. The frontal lobe conveys information on emotional behavior. The parietal lobe receives impulses from such sensory receptors from the skin such as pressure and pain. The temporal lobe is responsible for auditory impulses, which are received via auditory sensors inside the ear. The occipital lobe is the visual cortex, which displays information based on visual stimulation.
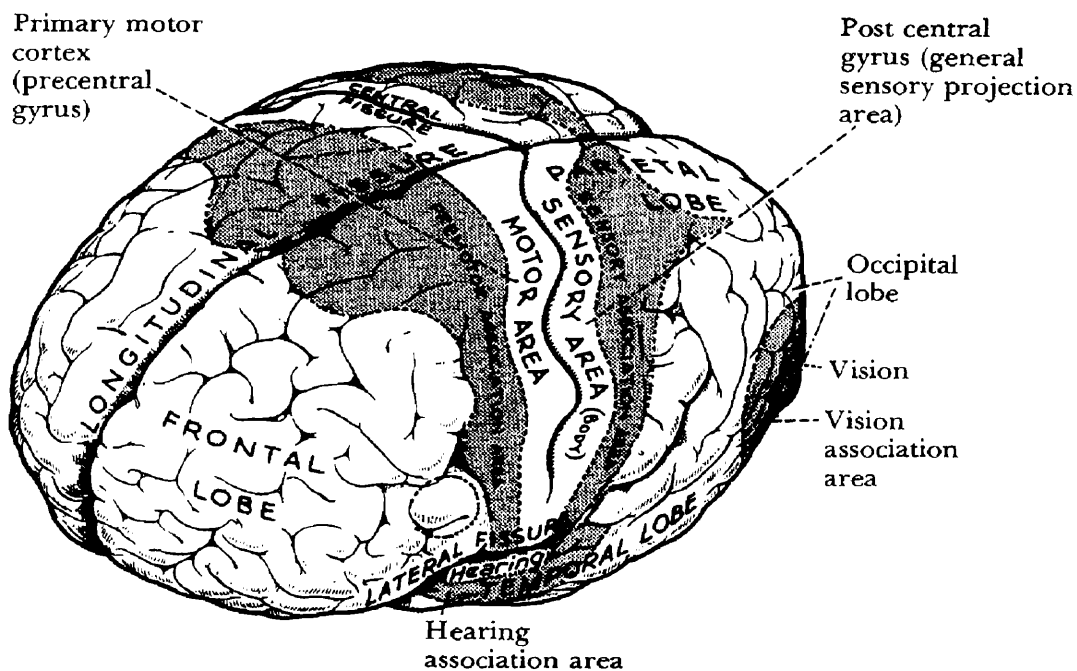
Figure 2.1 The cerebrum, showing the four lobes (frontal, parietal, temporal, and occipital), the lateral and longitudinal fissures, and the central sulcus[12].

2.3 Resting Rhythms

Brain activity is observed through a series of oscillating rhythms, which can be recorded from the exposed surface of the brain as well as the outer surface of the head. The intensity and pattern of these recorded potentials are determined by contributions due to excitation of various sections within the brain.
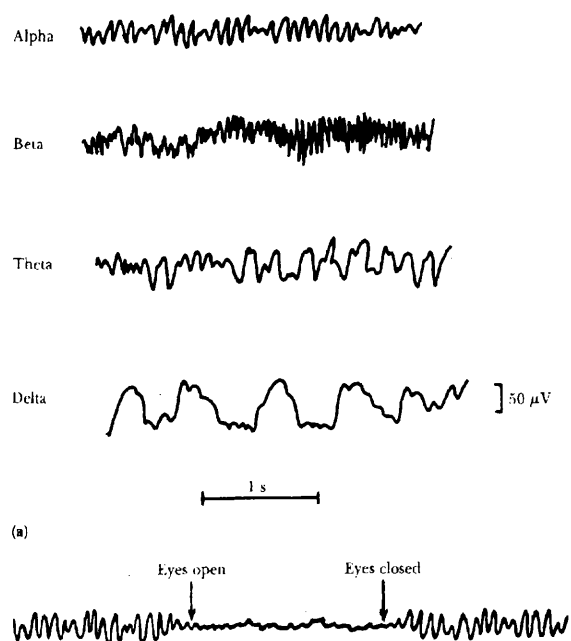
Figure 2.2 Examples of EEG [12].

The intensity of brain signals from the scalp can reach approximately $100\,\mu V$ with a range in frequency from 0.5 to 100 Hz. The degree of activity in the cerebral cortex has an important role in the brain signal response. Waveforms can contrast greatly between states of sleep and wakefulness. Irregularity in brain signals is a common factor in most recordings. Yet at other times, distinct patterns reveal vital information. In normal subjects, these distinct patterns can be classified into 4 different groups of brain signals: alpha, beta, theta, and delta rhythms.

Alpha rhythms occur at a frequency between 8 and 13 Hz. These signals are observed when the subject is in a resting, quiet state with eyes closed. They are observed most intensely in the occipital region, but can also be recorded at times in the frontal and parietal regions of the scalp. Alpha rhythms will disappear completely during states of sleep and mental activity.

Beta rhythms occur in the frequency range of 14 to 30 Hz, and sometimes are observed at 50 Hz during intense mental activity. They are frequently recorded in the parietal and frontal regions of the scalp and can be divided into 2 groups: beta I and beta II. Beta I waves behave like alpha waves in disappearing during intense mental activity, whereas Beta II waves appear during intense mental activity at a lower voltage level.

Theta rhythms occur between 4 and 7 Hz and can be recorded in the parietal and temporal regions of children as well as in adults during emotional stress or periods of disappointment. These waves can be created by exposing the subject to a pleasant stimulus and then removing the stimulus from the subject's sight. This effect results in approximately 20 seconds of theta rhythms.

Delta rhythms appear at frequencies below 3.5 Hz at infrequent times. They occur during deep sleep in infancy or in the presence of a serious organic brain disease. They occur solely within the cortex, independent of lower region brain activity.

In order for brain signals to occur, a large number of neurons must be synchronously activated to create an extracellular current strong enough to produce the potentials recorded on the cerebral surface. Synchronization can occur through long-lasting depolarization of the cell membranes or a summation of a number of shorter responses. Synaptic interconnections as well as extracellular field interactions are assumed to be responsible for such synchronization.

2.4 The Magnetoencephalogram (MEG)

Brain activity is typically characterized by measurement of electrical fields created by the brain's bioelectric sources. These time-varying bioelectric sources also create time-varying magnetic fields, which equally can be used to quantify the brain activity. The

magnetic fields generated from the cortex during alpha activity are approximately equal to 0.1 pT at a 5 cm distance from the surface of the scalp. These magnetic fields are extremely low in magnitude and pose great limitations in their detection and measurements. In comparison, the earth's magnetic field is roughly one hundred million times stronger at approximately $50\,\mu T$. Recent advances in the field of superconductivity have made these measurements possible. These advances have led to devices such as the Superconducting Quantum Interference Device (SQUID) magnetometer [12]. This is a magnetic-field measuring apparatus which uses a superconducting effect at liquid helium temperature to produce a measuring sensitivity on the order of 0.01 pT. Background fields such as the earth's magnetic field can be eliminated using a gradiometer technique (differential coils).

Magnetic field recordings offer a number of advantages:

- the differential nature of the coils used in magnetic field measurements permits to obtain response from the nearest stimuli as well as eliminate the contributions from the remaining distant sources.

- such measurements can also be used to determine the depth of the stimuli,

- non-contact measurements offer non-invasive characteristics.

Continuing studies are urged on by these types of advantages, which in return are limited by the complexities of recording such signals. The squid, for example, can require over 100 channels for recordings in order to measure the field distribution over the surface of the scalp and could be prohibitively expensive.

CHAPTER 3

INSTRUMENTATION

The performance of an electroencephalogram filter must incorporate several features in order to capture and condition the recorded signal. It must provide exceptional low noise performance in order to differentiate the brain signal, which can be as small as $100\,\mu V$ in scalp recordings from the noise. The filter must also provide the proper isolation from external power sources in order to insure the safety of the subject. Band-pass capabilities must eliminate 60 Hz noise as well as other unwanted signals. Finally, the filter must amplify the signal with clarity and precision, thereby extracting the desired signal and minimizing unwanted noise.

3.1 Filter Construction

Previous research has shown that the brain frequency range of interest in detecting a measurable difference between a subject having their eyes open as opposed to closed is centered around 10 Hz [13]. Therefore, the initial goal in filter construction was set to design a low noise high gain filter with a center frequency of 10 Hz and a bandwidth of 2 Hz. Taking these necessities into consideration, the step-by-step procedure was followed:

- the low noise characteristics would be accomplished through the selection of high quality op-amps,

- the initial estimates for the gain and bandwidth were provided through a filter estimation software, which yielded the required order and Q factors for each stage of the filter. Taking into consideration the high Q needed per stage in order to provide the narrow bandwidth with high gain, proper configuration was selected for the band-pass stages of the filter,

10

- all other features including input/output impedance, isolation, and additional output

    gain were introduced and implemented in the circuit layout,

- the printed circuit board layout was created via AutoCad14,

- the printed image was then transposed onto a copper board,

- a solution was used to dissolve the copper leaving only the circuit route present,

- the circuit board was then drilled,

- the IC chips were then mounted on and soldered,

- the circuit was then tested with a low frequency function generator centered around 10

    Hz .

3.2 Biquadratic Filter Circuits

Due to strict requirements of high gain and narrow bandwidth, it was imperative to use

circuit topologies which yield high Q factors. The biquadratic filter configuration

provides stability and easy frequency tuning. Although it requires more components per

stage, it yields much greater Q-factors than most 2nd-order filter configurations. The quad

op-amp chip can be used in providing a single stage with minimal external components.

The name biquad is derived from the circuit's description, which can be represented as

the ratio of two quadratic expressions.

3.2.1 Analysis

The high-pass filter transfer function is used as a starting point in the analysis:

$$H\left(jw\right) = H\left(j\omega\right) = \frac{K\omega^2}{-\omega^2 + \left(\frac{\omega_0}{Q}\right)j\omega + \omega_0^2} \tag{1}$$

Substituting $s = j\omega$ into (1) leads to

$$H(s) = \frac{-Ks^2}{s^2 + \left(\dfrac{\omega_0}{Q}\right)s + \omega_0^2} \tag{2}$$

Normalizing the angular frequency to $\omega_0 = 1$ rad/s reduces (2) into the following expression:

$$H(s) = \frac{-Ks^2}{s^2 + \dfrac{s}{Q} + 1} \tag{3}$$

Expression (3) can be re-written as:

$$H(s) = \frac{V_o}{V_i}(s) = \frac{-K}{1 + \dfrac{1}{Qs^2} + \dfrac{1}{s^2}} \times \frac{\left(\dfrac{P}{K}\right)}{\left(\dfrac{P}{K}\right)} \tag{4}$$

which is equivalent to:

$$V_0 = -P \tag{5.a}$$

and
$$V_i = \frac{P}{K} + \frac{P}{K}\left(\frac{1}{Qs}\right) + \frac{P}{K}\left(\frac{1}{s^2}\right) \tag{5.b}$$

or
$$P = KV_i - \frac{P}{Qs} - \frac{P}{s^2} = KV_i + \frac{V_o}{s} + \frac{V_o}{s^2} \tag{5.c}$$

The output P = - Vo is the sum of the three input voltages as shown in Figure 3.1.
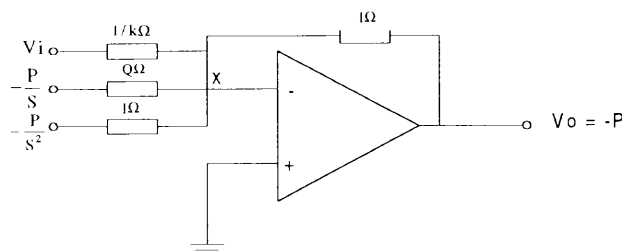
Figure 3.1 Simple summing amplifier.

In producing this output, a single and cascading integrator circuit will be needed in order to provide the $\frac{1}{s}$ and $\frac{1}{s^2}$ effects. The realization of the basic biquad circuit is shown in Figure. 3.2
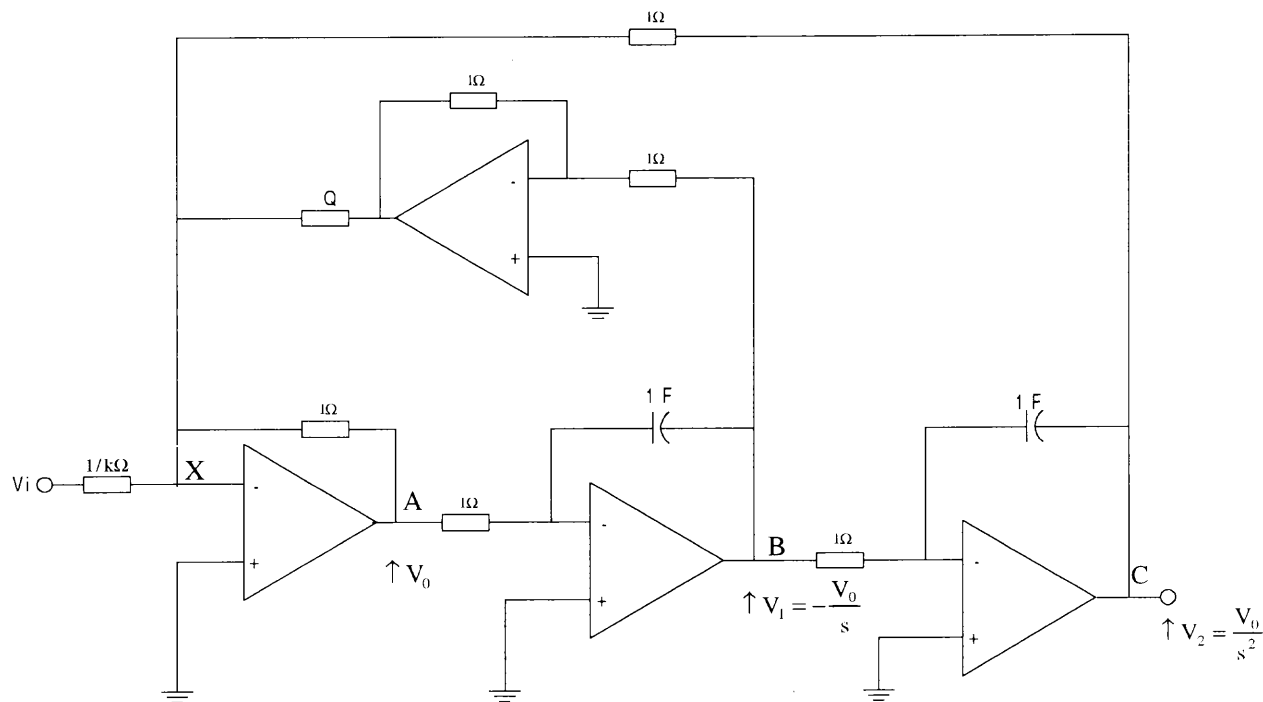
Figure 3.2 Circuit realization for the basic biquad.

The second order transfer function is synthesized by cascading two identical integrator circuits. The summation of the three quantities is achieved at node X, which occurs at the input of the first op-amp. Note that the output at node B is inverted before reaching node X.

Nodal analysis at node X yields

$$\left(0 - V_i\right)K + \left(0 - V_o\right) + \left(0 - \frac{V_o}{s}\right)\frac{1}{Q} + \left(0 - \frac{V_o}{s^2}\right) = 0 \tag{6}$$

which simplifies into

$$-KV_i = V_o\left(1 + \frac{1}{Qs} + \frac{1}{s^2}\right)$$ (7)

yielding

$$\frac{V_o}{V_i} = \frac{-Ks^2}{s^2 + \frac{s}{Q} + 1}$$ (8)

The circuit described above is useful in realization of a high-pass function at node A.

Further, noting the following relations

$$V_1 = -\frac{V_0}{s}, \quad V_2 = \frac{V_0}{s^2} = -\frac{V_1}{s}$$ (9)

and applying them at node B, leads to

$$\frac{V_o}{V_i} \times \frac{V_1}{V_o} = \frac{V_1}{V_i} = \frac{-Ks^2}{s^2 + \frac{s}{Q} + 1} \times \left(\frac{-1}{s}\right) = \frac{Ks}{s^2 + \frac{s}{Q} + 1}$$ (10)

which is also a band-pass function. Also, the transfer function at node C is expressed as

$$\frac{V_2}{V_i} = \frac{V_1}{Vi} \times \frac{V_2}{V_1} = \frac{Ks^2}{s^2 + \frac{s}{Q} + 1} \times \left(\frac{-1}{s}\right) = -\frac{Ks}{s^2 + \frac{s}{Q} + 1}$$ (11)

Equation (11) represents a low-pass function as well.

Since the band-pass features of the circuit are of interest in this thesis, one may eliminate one of the op-amps in the circuit by combining the operations of integration and summation as shown Figure 3.3.
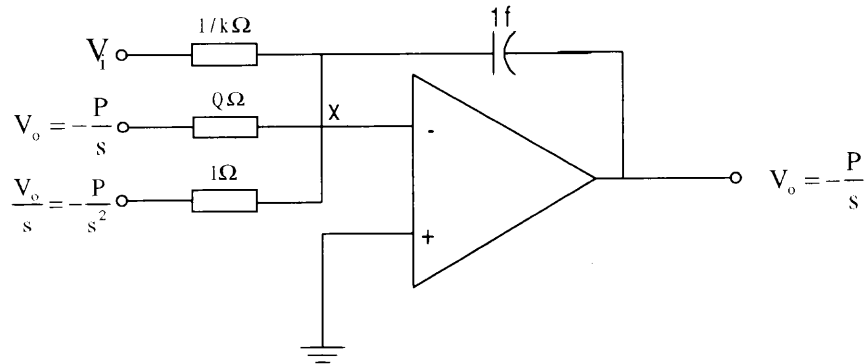
Figure 3.3 Summation and integration.

Nodal analysis at node X yields

$$(0 - V_i)K + (0 - V_o)\frac{1}{Q} + \left(0 - \frac{V_o}{s}\right) + (0 - V_o)s = 0 \tag{12}$$

Simplification of equation (12) yields

$$-KV_i = V_0\left(s + \frac{1}{s} + \frac{1}{Q}\right) \tag{13}$$

resulting in the transfer function at node B of Figure 3.3.

$$\frac{V_o}{V_i} = \frac{-Ks}{s^2 + \frac{s}{Q} + 1} \tag{14}$$

Equation(14) represents the band-pass function occurring at node A in the final circuit of

Figure 3.4. Once again, in realizing $\frac{V_0}{s}$, a further integrator is needed followed by an

inverter circuit in order to achieve the correct polarity.
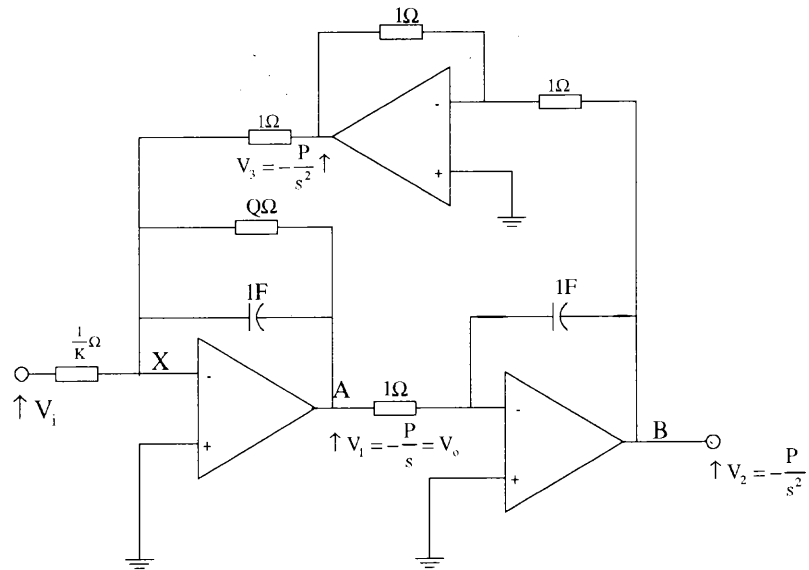
Figure 3.4 Circuit realization of low pass and band pass cases.

This circuit may then be modified to realize a positive-going band-pass output by re-arranging the op-amps as shown in Figure 3.5.

Which produces the transfer function

$$\frac{V_o}{V_i} = \frac{Ks}{s^2 + \dfrac{s}{Q} + 1} \tag{15}$$
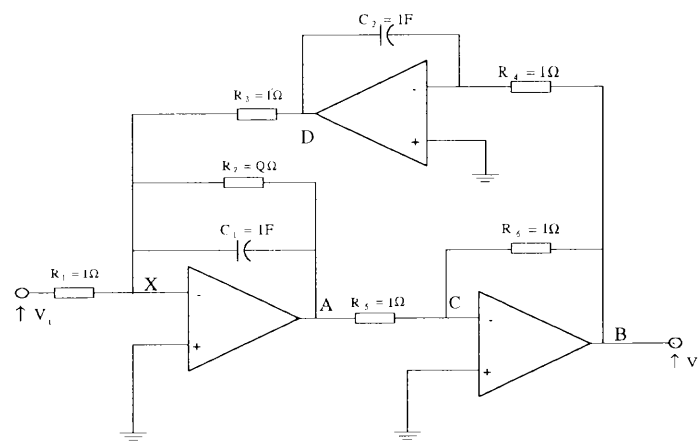
Figure 3.5 Biquad band pass realization.

Considering now the circuit with actual components and the following conditions:

C1= C2 = C and R4 = R5 = R6, nodal analysis at node X yields

$$\frac{V_i}{R_1} + \left(sC + \frac{1}{R_2}\right)V_A + \frac{V_D}{R_3} = 0 \tag{16}$$

Also, considering the following relations

$$V_C = -V_A,$$
$$V_D = -\frac{V_C}{sCR_4} = \frac{V_A}{sCR_4} \tag{17}$$

in (17) results in the band pass realization of

$$\frac{V_o}{V_i} = \frac{\dfrac{s}{CR_1}}{s^2 + \dfrac{s}{CR_2} + \dfrac{1}{C^2 R_3 R_4}} \tag{18}$$

Substituting s = jw into (17) yields

$$\frac{V_o}{V_i}(j\omega) = \frac{j\omega G \dfrac{\omega_0}{Q}}{-\omega^2 + j\omega \dfrac{\omega_0}{Q} + \omega_0^2} \tag{19}$$

where

$$\omega_0 = \frac{1}{\left(C^2 R_3 R_4\right)^{0.5}} \tag{20}$$

$$G = \frac{R_2}{R_1} \tag{21}$$

$$R_2 = \frac{Q}{C\omega_0} \tag{22}$$

$$R_3 = R_4 = \frac{1}{\omega_0 C} \tag{23}$$

For R3 made equal to R4.

The center frequency adjustment is performed by R3. R2 controls the filter's Q

adjustment, and R3 controls the center frequency gain. Figure 3.6 displays the Biquad

Bandpass Gain for Q values of 20, 50, and 100.
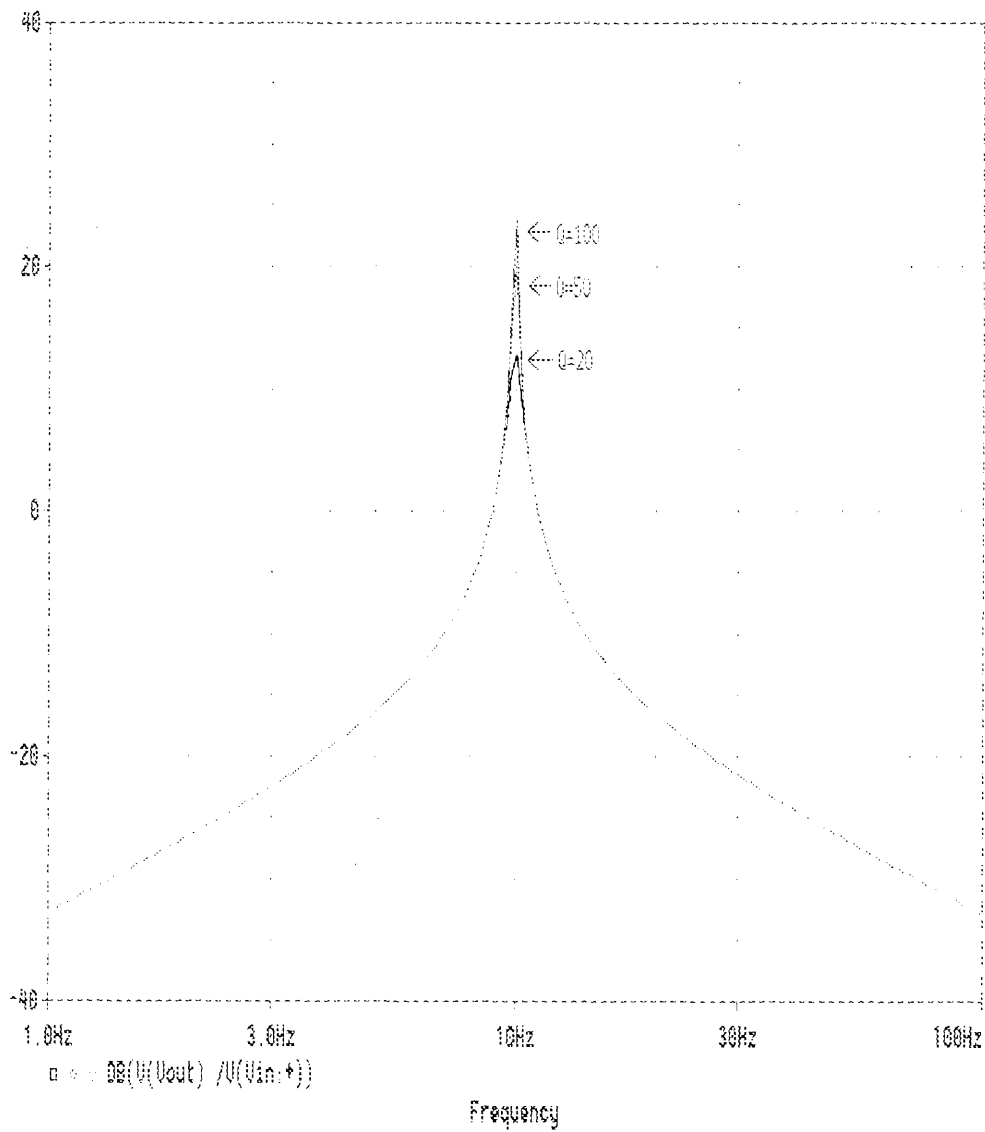
Figure 3.6 Biquad band pass gain for Q values of 20, 50, and 100.

3.3 Amplifier Setup

An amplifier was built initially in order to retrieve signals from the coil-based system.

There was no need for optical isolation within the amplifier because the coils were not in

contact with the subject. The next amplifier was designed for electrode inputs. Due to

contact with the subject, differential inputs and isolation circuitry was needed. Both

designs shared the same band-pass and output stages.

Stage 1 – Input

  - Coil-based sensing – Unity gain voltage-follower was used in order to provide high

    impedance for the single-ended input.

  - Electrode-based sensing – Differential inputs were derived through Burr-Brown's

INA101 Instrumentation Amplifier. The INA101 is specifically designed for low-level

signal amplification with all features such as high CMRR, high input impedance, and

adjustable gain.
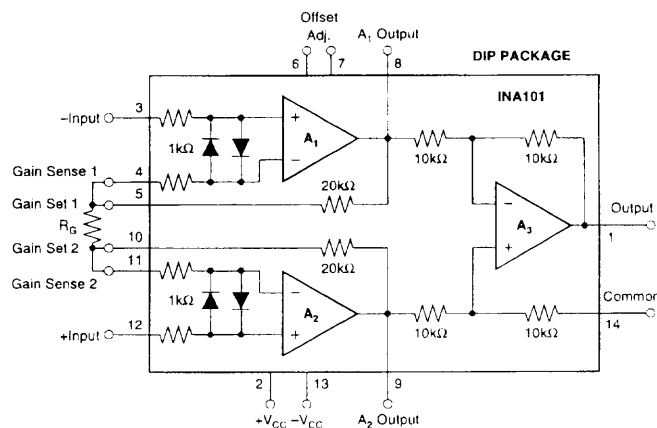
Figure 3.7 Schematic diagram of INA101 Instrumentation Amplifier.

Stage 2 – Isolation

This stage is a requirement for the electrode-based amplifier due to the direct connection

between the electrical circuitry and the subject. Analog Device's AD202 is a general

purpose, transformer-coupled isolation amplifier designed for a wide range of

applications including the measuring of input signals while eliminating any galvanic

connections. This industry standard isolation amplifier offers both signal and power

isolation in a single DIP package.
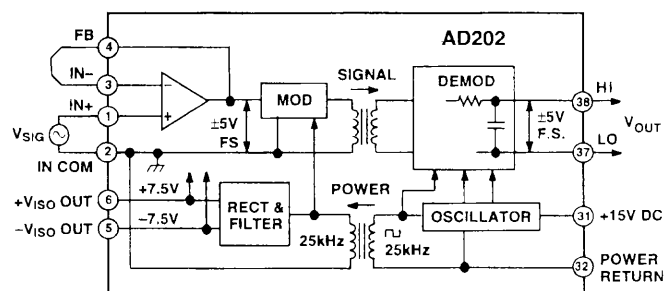
Figure 3.8 Functional block diagram of the AD202.

The AD202 is powered directly from a 15V supply. Features include bipolar 5V output

range, adjustable gain, 130 dB CMRR, and low power consumption. This stage comes

directly after the input stage, thereby isolating the subject from any leakage current from

the instrumentation.

Stage 3 – Biquad Filter / Amplifier

Signal conditioning takes place in this section. The coil-based amplifier uses 5

biquad band-pass stages centered around 10 HZ in order to achieve high Q and sufficient

gain. As previously explained, the biquad configuration is able to handle a Q-factor up to

100. Analog Device's OP-470 low-noise quad op-amps are used in order to provide

single-chip staging as well as low-noise capabilities. Desirable circuit performance was

achieved with the exception of a small amplitude internal oscillation, which could be

attributed to the number of filter stages. In order to eliminate such oscillations, the

electrode-based amplifier used 4 biquad band-pass stages as opposed to 5. Stage 3

amplification can provide a gain of approximately 60 dB with limitations due to the

inherent oscillations as well as saturation.

Stage 4 - Output

With the signal now conditioned and amplified, the output stage provides any final

amplification needed along with low output impedance. A non-inverting amplifier is used

in series with a voltage-follower in order to complete the circuit. At this point, only

minimal amplification is needed.

3.4 Data Acquisition and Analysis

Both data acquisition and analysis were performed on a Dell Windows 95 notebook

computer. The computer contained a Pentium processor with 233 MHz clock speed and

32.0 MB of RAM. The primary goal in instrument selection was to acquire and analyze

data in an accurate and efficient manner. The software tools utilized for this purpose were

National Instrument's Labview 5.1 and MATLAB 4.2, for data acquisition and

processing, respectively. Although, Labview offered data acquisition software as well as

processing capabilities, signal processing in MATLAB was preferred.

3.4.1 Acquisition

National Instrument's Labview 5.1 was used in conjunction with National DaqCard-

1200 as our data acquisition system. The DaqCard-1200 is an I/O PC card with eight

inputs, which can be connected as either eight single-ended or four differential inputs. Analog input ranges can vary from 0 to 10 volts (unipolar) or from –5 to 5 volts (bipolar). The DaqCard-1200, which slides into the PC Card slot, along with the I/O cable and connector, interfaces the analog input signal with the processor.

The Labview 5.1 software tool controls the DaqCard-1200 data acquisition card in collecting the analog data, and converting it into digital format for further processing by the MATLAB software. This task is accomplished through Labview's "Continuously Acquire to Spreadsheet File" virtual instrument. This program writes voltage scaled data continuously to a text file readable by spreadsheet programs. It allows parameter adjustments such as scan rate, buffer size, and number of scans to write at one time. A graph display allows real-time view of the input signal. Once a load file is created, the program begins collecting data within the created file. Data collection is terminated manually through a virtual stop button.

3.4.2 Data Analysis

In analyzing electroencephalogram signals, it is best suited to convert the acquired signal from the time to frequency domain due to the complexity and irregularity of its nature. MATLAB 4.2 offers a suitable variety of tools in order to create a frequency spectrum plot.

3.4.2.1 Fast Fourier Transform (FFT): The Fast Fourier Transform [14]is a signal processing technique which converts the time domain signal into the frequency domain. To implement FFT, the signal must be quantized at an appropriate sampling rate, preferably the Nyquist rate. In this thesis, alpha wave signals are within the 8 to 12 Hz

band. Therefore, a sampling frequency greater than or equal to 25 Hz would be theoretically sufficient. If signals harmonics must also be taken into consideration, the sampling rate must then be adjusted, accordingly. However, in our experimentation with Labview 5.1, an alaising effect was generated with sampling rates as high as 200 samples per second. This alaising was observed to be eliminated with a sampling rate of 600 samples per second. Therefore, the sampling rate was not only dictated by the recorded signal, but by introduction of the alaising effect due to Labview's data acquisition system as well.

3.4.2.2 Analysis of FFT: The FFT yields a series of terms describing the function in the frequency domain as a finite series of complex numbers where N = number of points in time that are included in the discrete time series. Recalling the Fourier transform definition as

$$F(\omega) = \int_{-\infty}^{+\infty} f(t) \cdot e^{-i \cdot \omega \cdot t} \cdot dt$$

or the discrete definition results in

$$\alpha_j = \frac{1}{N} \sum_{1}^{N} f_k \cdot e^{-i \cdot 2 \cdot \pi \cdot j \cdot \frac{k}{N}}$$

If time is changed to the amount t_0 the first of these two equations can be written as

$$F_{t_0}(\omega) = \int_{-\infty}^{+\infty} f(t + t_0) \cdot e^{i \cdot \omega \cdot t} \cdot dt$$

$$= e^{-i \cdot \omega \cdot t_0} \cdot \int_{-\infty}^{+\infty} f(\tau) \cdot e^{i \cdot \omega \cdot \tau} \cdot d\tau$$

$$= e^{-i \cdot \omega \cdot t_0} \cdot F(\omega)$$

In the second case it is equivalent to altering the subscript k by $\dfrac{t_0}{N}$

$$\alpha_{j,t_0} = e^{-2\cdot\pi\cdot i\cdot t_0/N} \cdot \alpha_j$$

$F(\omega)$ and α_j are shifted by t_0, but their absolute values remain the same

$$\left|F_{t_0}(\omega)\right|^2 = \left|F(\omega)\right|^2$$

$$\left|\alpha_{j,t_0}\right|^2 = \left|\alpha_j\right|^2$$

The power spectrum is the expected value of $\left|\alpha_j\right|^2$.

MATLAB offers an FFT function which executes the Fast Fourier Transform. A program called "spc_plt" utilizes this function and then graphs the recorded results. The graph displays the frequency component on the x-axis and the power component on the y-axis. This program is included in Appendix B.

CHAPTER 4

EXPERIMENTAL RECORDINGS AND RESULTS

The basic purpose of our recordings was to observe a measurable difference between the mental state in which the subject's eyes are open as opposed to being closed. Two different instrumentation approaches were used to detect this difference:

- electrode-based sensing,

- coil-based sensing.

In each method, recordings would then be separated into two parts by utilization of a:

- commercial biomedical amplifier,

- biomedical amplifier designed and built in this work. Results would therefore dictate the performance of the recording method as well as the performance and comparison of both instruments.

4.1 Electrode-Based Recordings

This experiment involved the connection of electrodes to the subject in an attempt to record brain activity. The subject was observed for a set period of time (approximately 1 minute) in order to obtain a measurable difference between the mental state of eyes opened and eyes closed. Two different amplifiers were used in retrieving the signal; the first being a commercial amplifier, and the second one developed was specifically to be used in this thesis. Data was then collected and analyzed.

4.1.1 Hardware and Software Tools

The following hardware instruments and software tools were used:

- Flextrodes – connecting device via gold electrodes.

- Amplifiers – (a) Gould Universal Amplifier – commercial differential amplifier

providing high input impedance and low noise characteristics,

(b) Biquad Filter / Amplifier – Differential amplifier designed for this

thesis.

- LabView 5.1 / DaqCard 1200 – data acquisition card.

- MATLAB – signal processing.

4.1.2 Electrode Placement

The International Federation 10-20 system shown in Figure 4.1 was followed to monitor

the EEG signal acquisition.

Figure 4.1 The International Federation 10-20 system for electrode placement in EEG.

This system uses anatomical landmarks in standardizing the electrode placement. As

stated earlier, the occipital region, located at the back of the head, corresponds to the

primary visual cortex. Eye reactions to different levels of light evoke large electrical

potentials measurable using electrodes placed over this region of the cortex. Therefore,

initial states of drowsiness could be detected by monitoring the EEG signals produced

from the occipital region of the cortex. Also, electrodes placed in the occipital region disregard common muscle artifact seen in frontal cortex activity. An observation of an epileptic study done at St. Barnabas Hospital in Livingston was able to confirm this information and provide insight to the electrode placement procedure followed in this thesis.

The differential amplifier requires a separate ground connection along with differential inputs to the following three types of electrode connections:

  - between each member of a pair (bipolar),

  - between one monopolar lead and a distant reference electrode,

  - between one monopolar lead and the average of them all.

The connections for this thesis required the monopolar lead Oc1, located in the occipital region of the cortex, along with Cz, as the distant reference electrode. Cz, located at the center-top of the cortex, proved to be a stable ground. The right earlobe was also used as the amplifier ground.

4.1.3 Skin Preparation

Skin preparation is critical in obtaining valid results in clinical EEG. EEG electrodes are small in dimension, and must be properly affixed to the scalp with minimal disturbance. The scalp must first be prepared by cleaning the area with alcohol. Next, an abrasive skin preparation gel (Nuprep) is used on the attached surface in order to insure a clean connectivity. Finally, a conductive paste (Ten20 Conductive) is used between the electrode and skin surface. The electrodes must then be secured in a fixed position in order to insure valid recordings. Such an electrode was used in obtaining ground connectivity through placement on the earlobe.

4.1.4 Flextrodes

A device called the flextrode, which offers a simple, clean, gel and paste-free electrode connection was used in order to avoid the complexities of electrode placement and skin preparation. The device uses a standard gold cup electrode encased in a plastic retainer. This plastic retainer is then inserted into a headband, which has hole configurations correlating to the I.F. 10-20 system. Two headbands are connected. The first is connected as a standard headband, allowing recording in the front and rear portions of the scalp. The second headband, which is worn across the top-center portion of the scalp, allows recordings to be done on the center portion of the scalp Each gold electrode is wrapped in a cotton swab within the plastic retainer. To provide conduction between the scalp and the electrode, the wrapped electrode is submerged in a saline-water solution. The cotton absorbs the saline-water solution and provides a moist contact for hours. This eliminates the need for glue and paste. The headband provides a secure and precise connection.

4.1.5 System Connection

A total of four subjects were tested individually. The subject was seated in a chair and prepared for electrode placement. Nuprep was applied to the right ear and then followed by an ear clip containing the Ten20 Conductive gel, which attaches the ear clip and provides the amplifier ground. The electrodes were then submerged into a saline-water solution and affixed into the Op1 and Fz slots in the headbands. These electrodes provided the inputs for the differential amplifier. The flextrode, now containing the conductive electrodes, was placed onto the subject's head in proper alignment with the I.F. 10-20 system. The flextrode output terminals were then fed into the amplifier. The amplifier in return forwarded the acquired signal to the notebook computer via the DaqCard 1200 data acquisition board.

4.1.6 Protocol

Each subject was recorded for a total of 4 one-minute session. The first two sessions

utilized the Gould Universal Amplifier, while the final two sessions utilized the Biquad

filter/amplifier. Each set of three sessions occurred as followed:

- eyes open 1-minute.

- eyes closed 1 minute.

Data was collected through the DacCard-1200 acquisition board attached to a Dell

notebook computer. The acquisition software used was Labview 5.1. The virtual

instrument " Continuously Acquire to Spreadsheet File " was used to collect data in text

format. MATLAB's frequency spectrum program was then used to analyze the data.

Samples were acquired at 600 samples per second in order to avoid alaising.

4.2 Electrode-Based Results

The measured and analyzed results validated that:

- a difference in signal level between both cases of eyes opened and eyes closed could

    be distinguished,

- the biquad differential amplifier worked equivalently in comparison to the commercial

differential amplifier. MATLAB's frequency spectrum plot confirmed the power and

frequency components of the recorded brain signals. Both amplifiers clearly

distinguished the difference in signal power between the cases of eyes open and eyes

closed. With eyes opened, all results clearly show little or no amount of alpha wave

production. With eyes closed, all results display an increase in alpha wave production

around 10 Hz.

Figures 4.2 through 4.5 display the frequency spectrum acquired from EEG analysis through utilization of the Gould Universal Amplifier for each subject, respectively. Subject A in Figure 4.2 showed a measurably stronger production of alpha rhythms with eyes closed as opposed to open. Subject B in Figure 4.3 showed a measurably stronger production of low-level beta rhythms with eyes closed as opposed to open. This may have been the result of greater mental activity due to stress. Subject C in Figure 4.4 showed a measurable difference in alpha rhythm production with eyes closed as opposed to open. Subject D in Figure 4.5 showed a measurably stronger production of alpha rhythm with eyes open as opposed to closed.

Figure 4.6 through 4.9 display the frequency spectrum acquired through EEG analysis through utilization of the Biquad Filter / Amplifier. Subjects A and C in Figures 4.6 and 4.8 each show a noticeable difference in alpha rhythm production with eyes closed as opposed to open. Subjects B and D in Figures 4.7 and 4.9 show greater signal strength differences in alpha rhythm production with eyes closed as opposed to open on the scale of approximately 40 and 7 times greater, respectively. The observed shift from the 10 Hz region into the 15 Hz region for Subject B could not have been observed here since the system is capable of detecting signal activity in the 10 Hz region only.
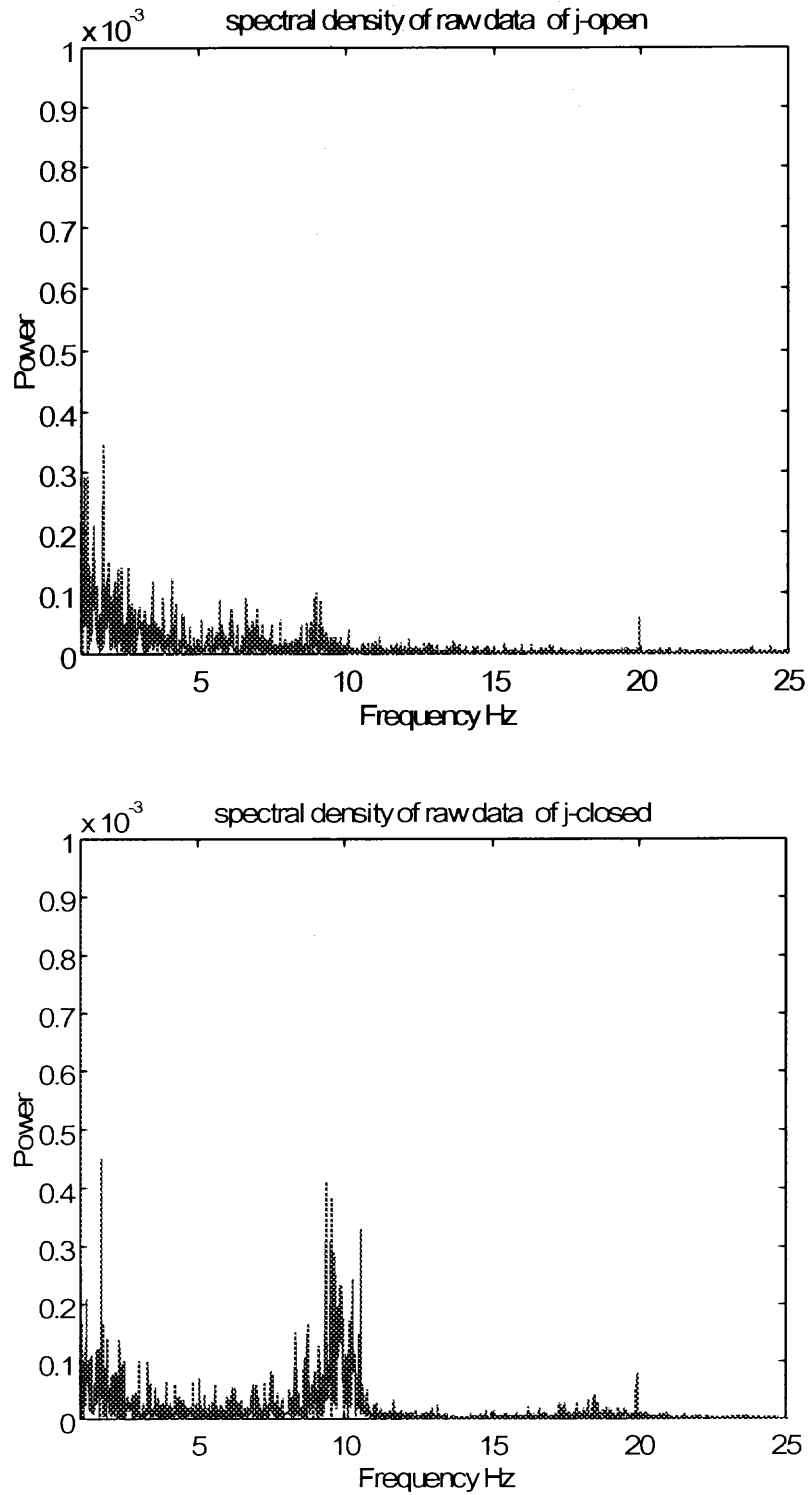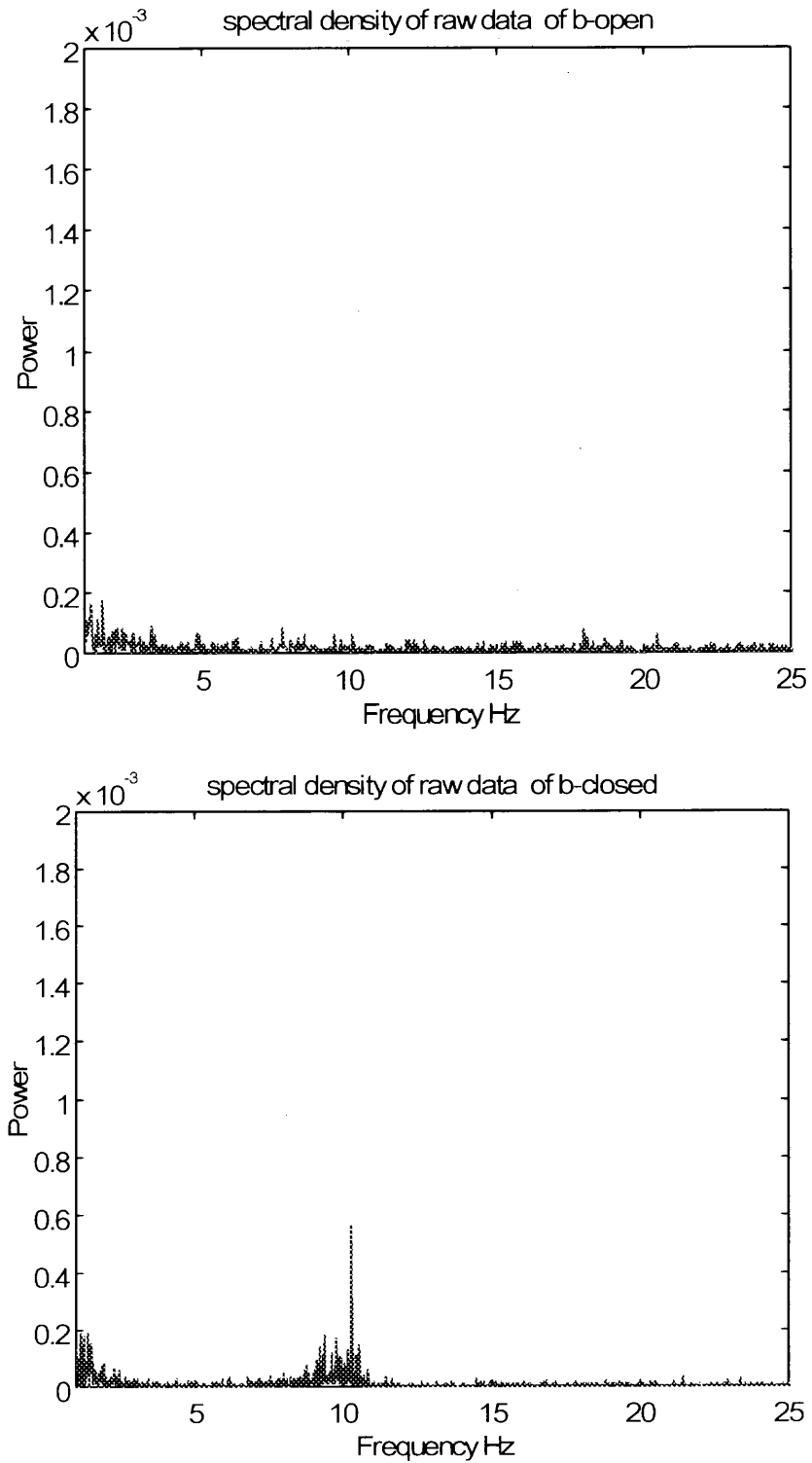
Figure 4.2 Frequency spectrum of subject A utilizing the Gould Universal Amplifer.
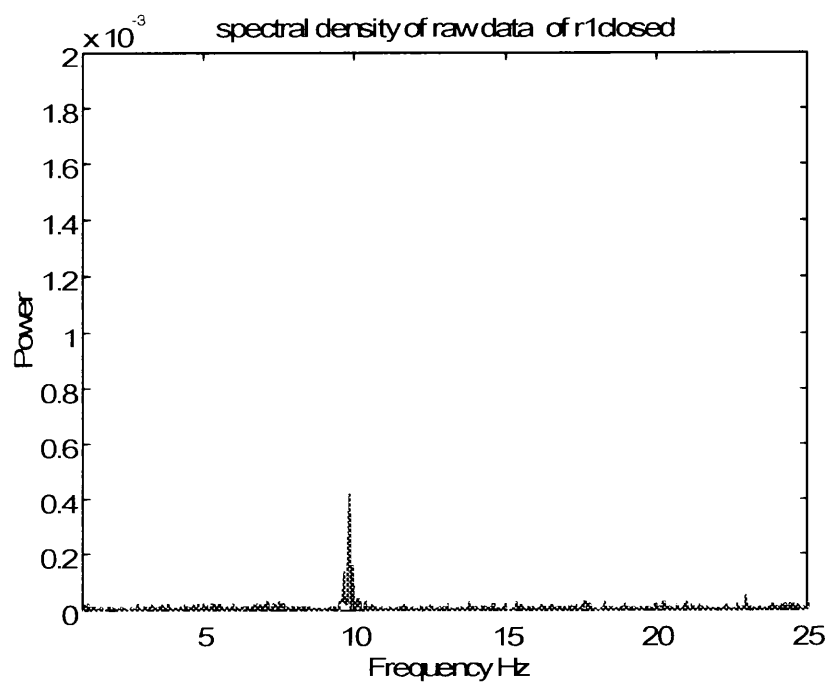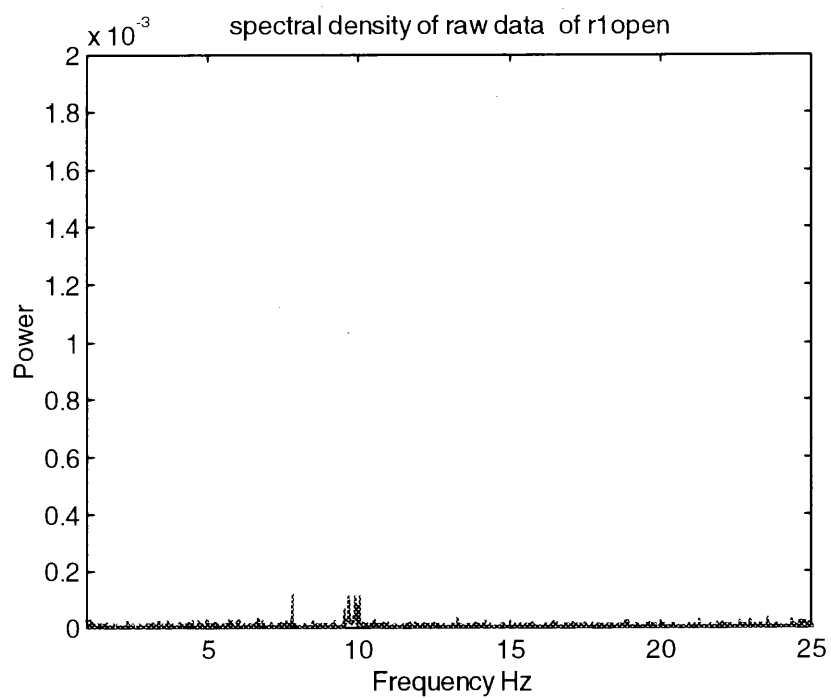
(a) eyes open
(b) eyes closed
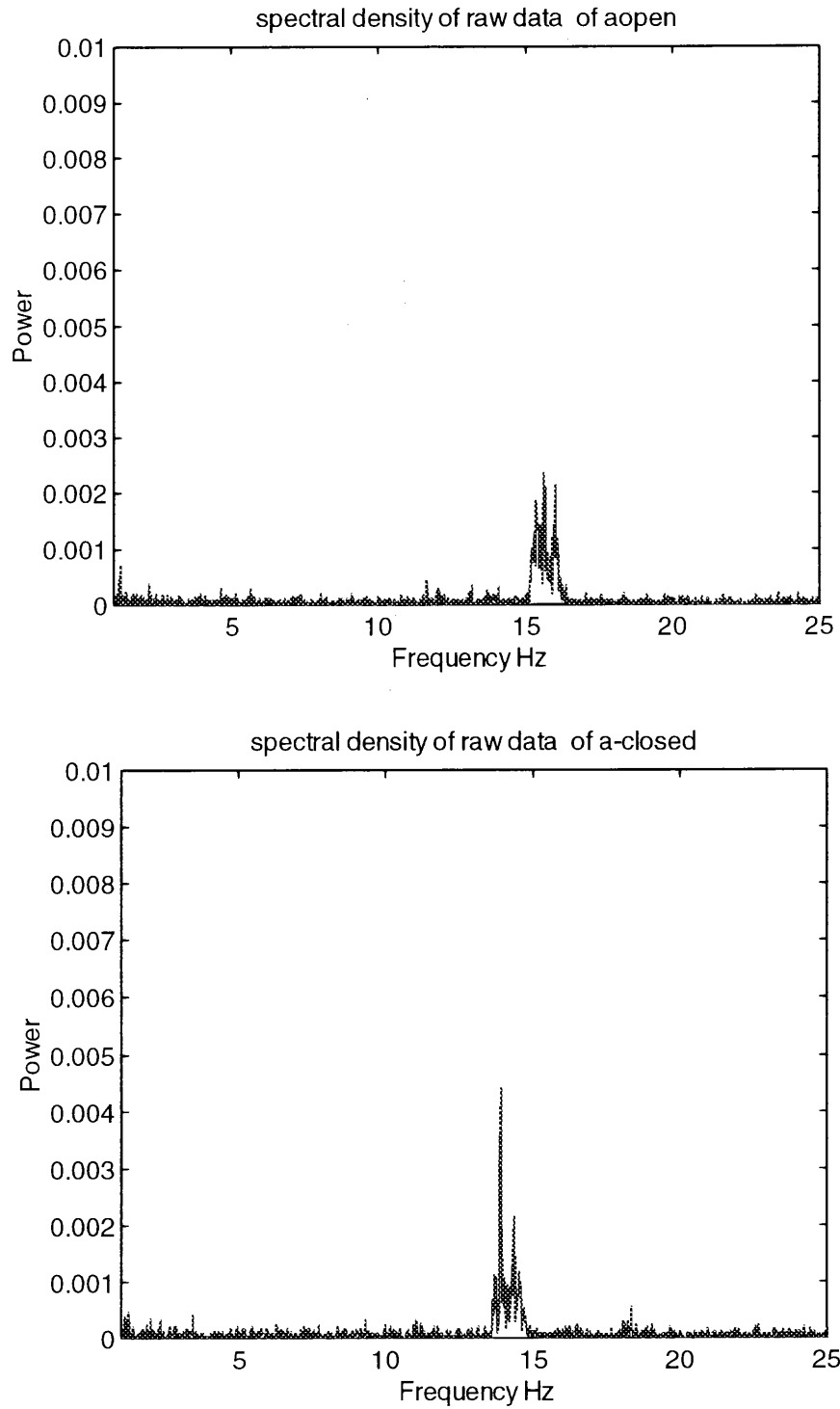
Figure 4.3 Frequency spectrum of subject B utilizing the Gould Universal Amplifier.
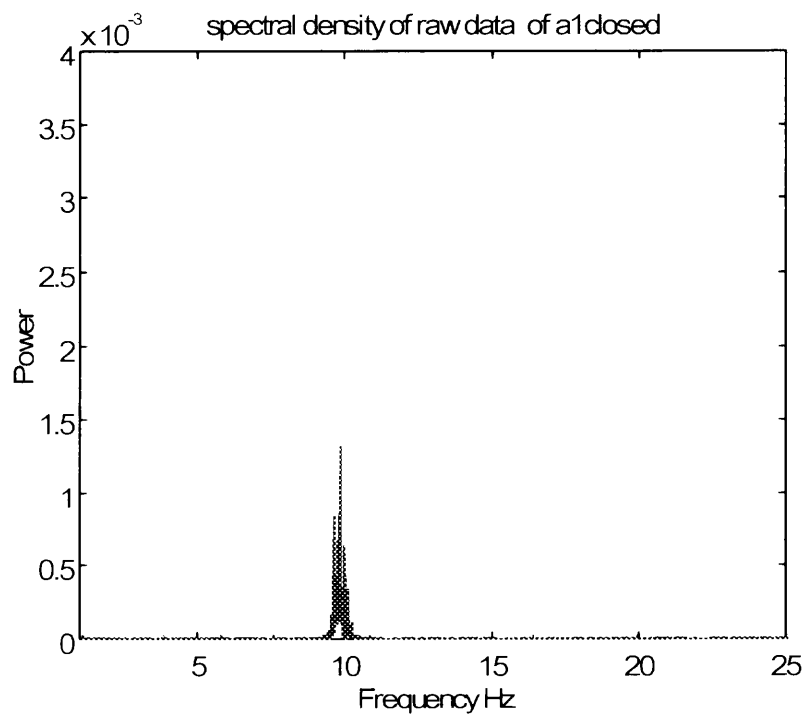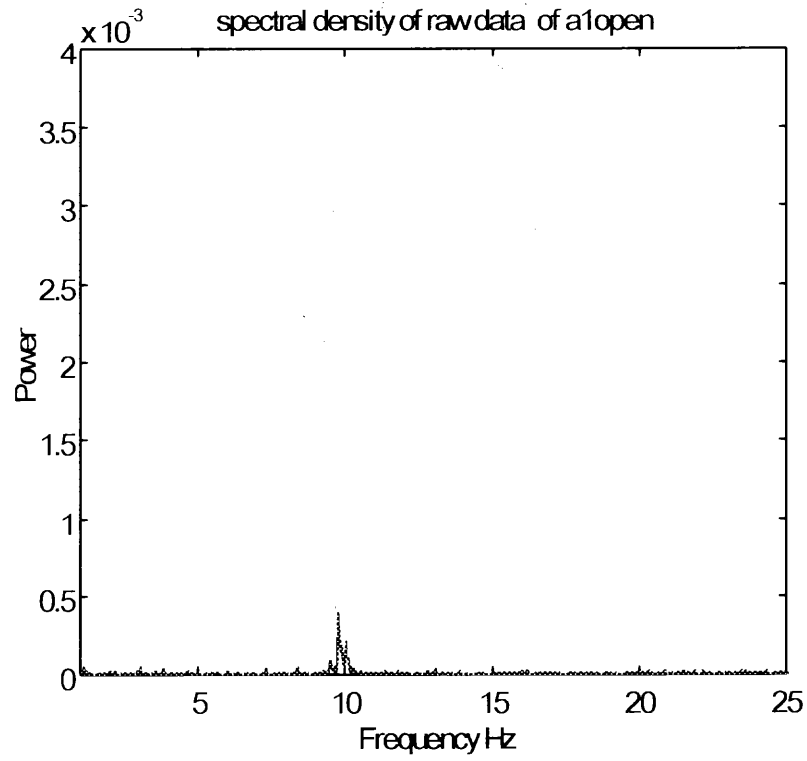
(a) eyes open

(b) eyes closed

Figure 4.4 Frequency spectrum of subject C utilizing the Gould Universal Amplifier.
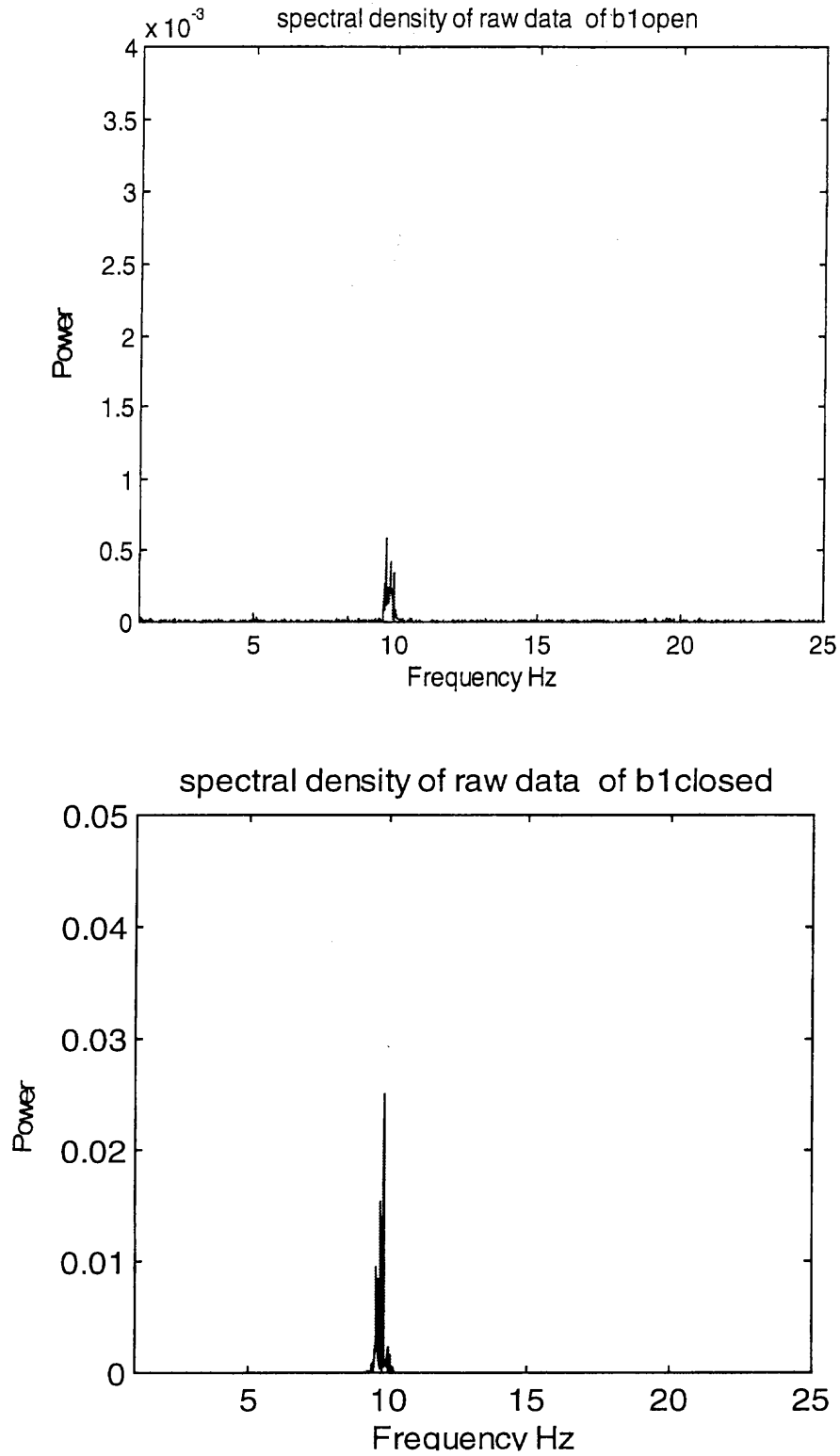
(a) eyes open
(b) eyes closed

Figure 4.5 Frequency spectrum of subject D utilizing the Gould Universal Amplifier.

    (a) eyes open

    (b) eyes closed

Figure 4.6 Frequency spectrum of subject A using the Piqued Amplifier.
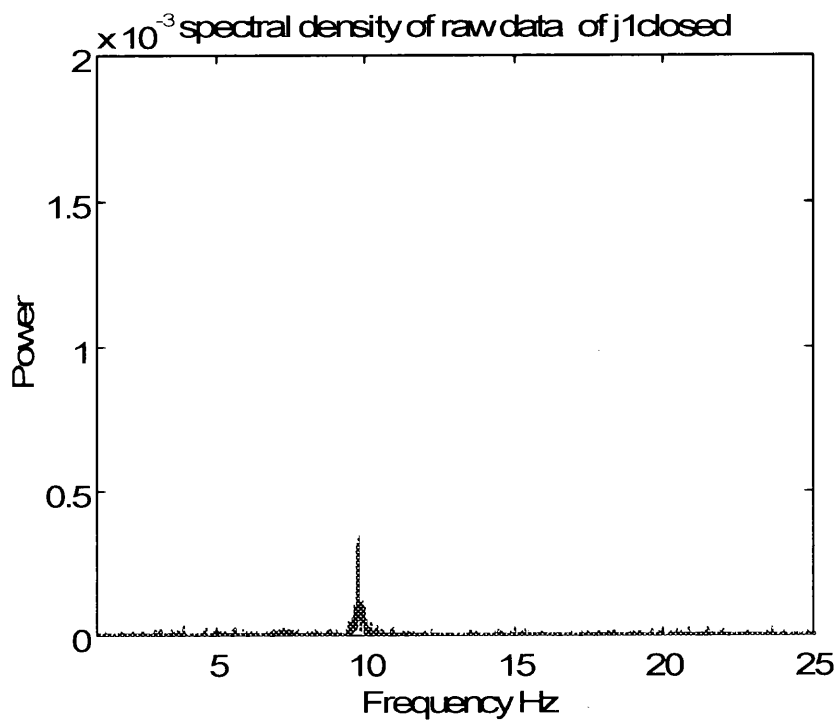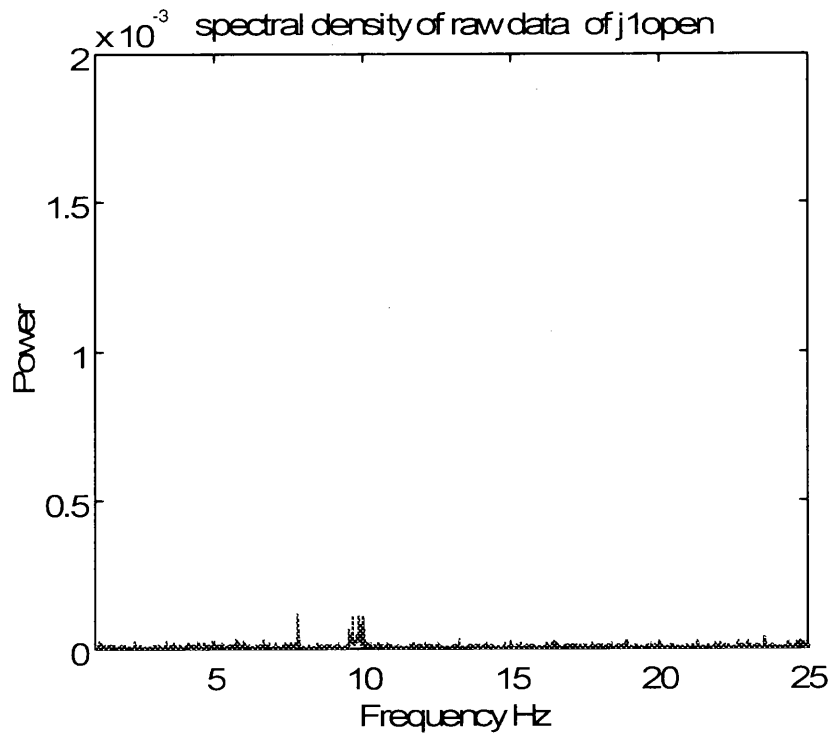
(a) eyes open

(b) eyes closed

Figure 4.7 Frequency spectrum for subject B utilizing the Biquad Amplifier.
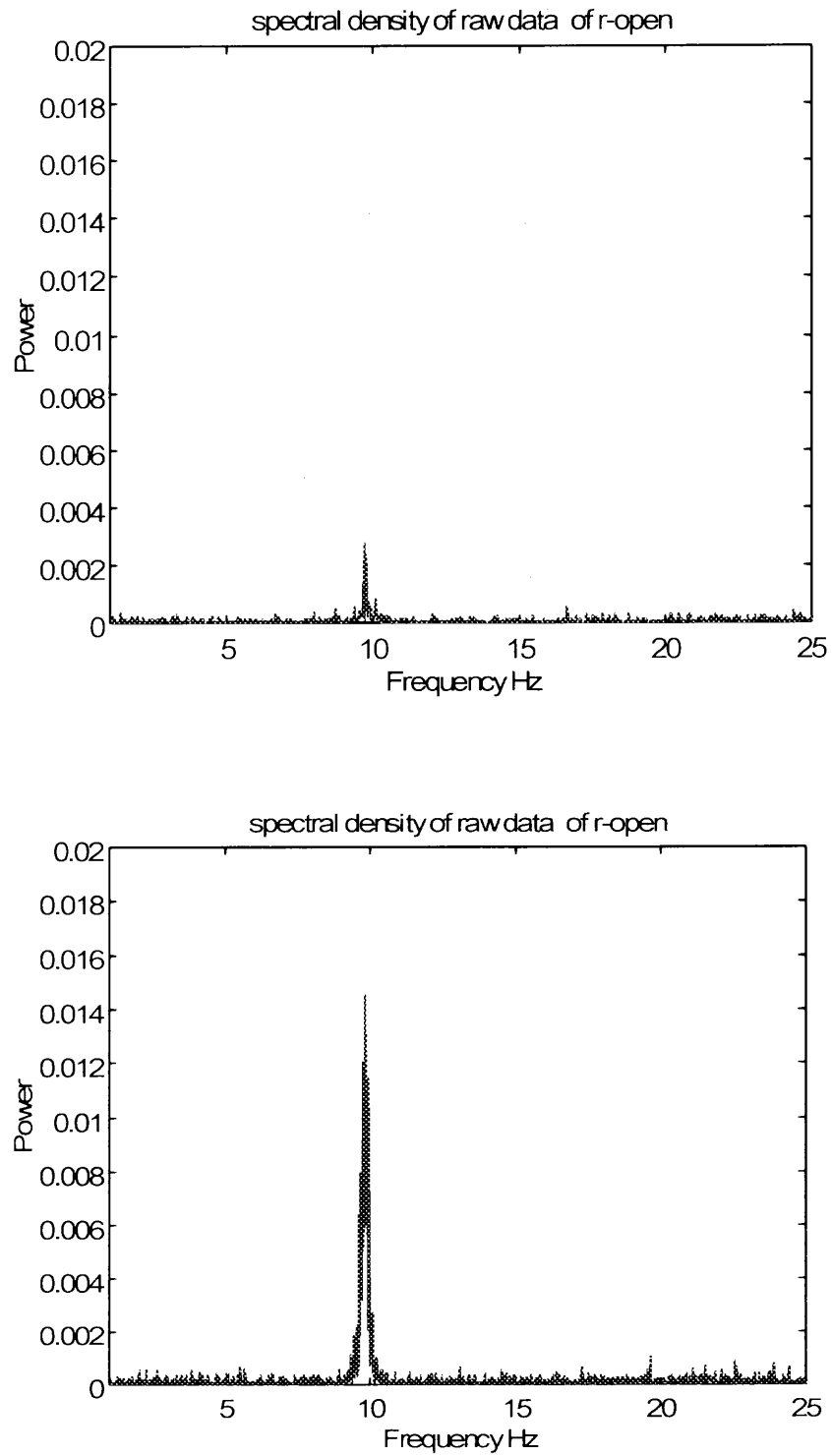
(a) eyes open
(b) eyes closed

Figure 4.8 Frequency spectrum of subject C utilizing the Biquad Amplifier.

(a) eyes open
(b) eyes closed

Figure 4.9 Frequency spectrum of subject D utilizing the Biquad amplifier.

(a) eyes open
(b) eyes closed

4.3 Coil-based Recordings

This experiment involved the use of two coils in a differential combination in an attempt to record the subject's brain activity. The subject was observed for a set period of time (approximately 1 minute) in order to obtain a measurable difference between the mental states of eyes opened and eyes closed. Once again, two different amplifiers were used in retrieving the signal; the first being a commercial Gould amplifier, and the second one was a biomedical amplifier designed for this work. Data was then collected and analyzed.

4.3.1 Hardware and Software Tools

- two 80,000 turn coils – differential mode measuring apparatus

- Amplifier – (a) Gould Universal Amplifier,

        (b) Biquad Filter / Amplifier – Differential amplifier designed for this

        project,

- Labview 5.1 / DaqCard 1200 – data acquisition,

- Matlab – frequency analysis.

4.3.2 Coil Placement

Two 80,000 turn coils were used to record each subject's brain activity. As in the case of the electrode-based recordings, we targeted the occipital region of the cortex as the area of measurement due to the region's visual-reacting capabilities. The coils were connected in a differential mode in order the measure the difference of currents induced in each coil. Theoretically, a significant difference in coil current during subject measurements would be attributed to an induced current created by the subject's brain signals. Coil positioning was initially varied in an attempt to produce maximum coil difference. Variance in coil positioning included:

- distance between the two coils,

- placement behind the subject's head.

Ultimately, the coils were distanced by approximately 1 foot and placed with the subject's head directly in front of one of the coils only. The coil distancing created no relevant difference. However, the subject's placement was critical in measuring the difference between the two coils. The greater the effect of induced current on one coil, the greater the difference between the two coils.

4.3.3 System Connection

Four subjects were tested individually using both amplifiers. The subject was seated in a chair directly in front of the two coils. One of the coils was then aligned with the occipital region of the scalp and placed as close as possible to the subject without creating direct contact. The second coil was kept approximately 1 foot away from the subject's head. The coil inputs were then fed into the amplifier. The amplifier in return sent the signal to the notebook computer via the DaqCard-1200 data acquisition board.

4.3.4 Protocol

Each subject was recorded for a total of 4 one-minute sessions. The first two sessions utilized the Gould Universal Amplifier, while the final two sessions utilized the Biquad filter / amplifier. Each set of three sessions occurred as followed:

- eyes open , 1-minute,

- eyes closed 1-minute.

Data was collected through the DaqCard-1200 acquisition board attached to a Dell Pentium notebook computer. The acquisition software used was Labview 5.1. The virtual instrument "Continuously Acquire to Spreadsheet File" was used to collect data in text

format. MATLAB's frequency spectrum program was used to analyze the data. Samples were obtained at 600 samples per second in order to avoid alaising.

4.4 Coil-Based Results

The results were unable to validate a difference in signals between both cases of eyes opened and eyes closed. In each case, utilizing the commercial amplifier as well as designed amplifier, results proved inconclusive. Most probably, induced currents were significantly buried in noise, hence resulting in insignificant changes. Sensitivity of the amplifiers was not adequate to capture these small changes.

In utilizing the Gould Universal Amplifier, a signal difference between states of eyes opened and eyes closed was unobtainable during each session. The variance of the coil as well as the subject's placement proved inconclusive. A lock-in amplifier was used at the output stage in an attempt to retrieve a signal. These results also proved inconclusive.

In utilizing the designed single-ended differential amplifier, a slight oscillation effect from the amplifier was observed. This effect may have been attributed to poor soldering or the multi-staging high gain band-pass sections. In any case, the oscillatory effect was minimal and presented only a minute degradation in the performance of the amplifier. Results once again proved inconclusive.

Figures 4.10 and 4.11 represent Subjects A and B EEG response to coil-based sensing. Both figures failed to display a measurable difference between the cases of eyes open and eyes closed. In comparison to Figure 4.12, which represent the EEG coil-based sensing with no subject involved, it is reasonable to assume that the small amount of signal received in the 10 Hz range in each case can be attributed to the slight internal oscillation of the amplifier. However, increase signal activity in Figure 4.10 compared to

results in the absence of a subject in Figure 4.12 may suggest that either the presence of a

subject was detected or that the presence of a subject caused an increase in internal

oscillations within the system.
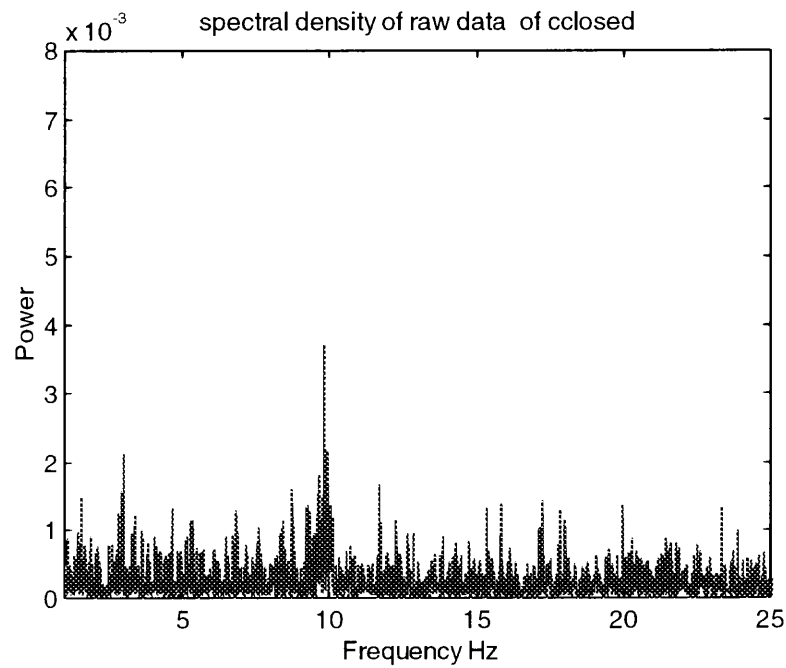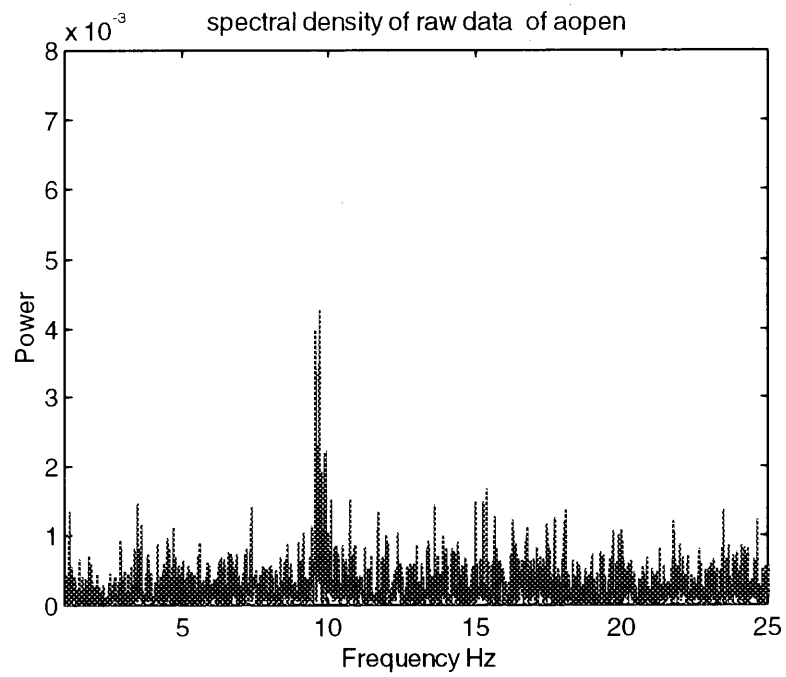
Figure 4.10 Frequency spectrum of Subject A through coil-based sensing.
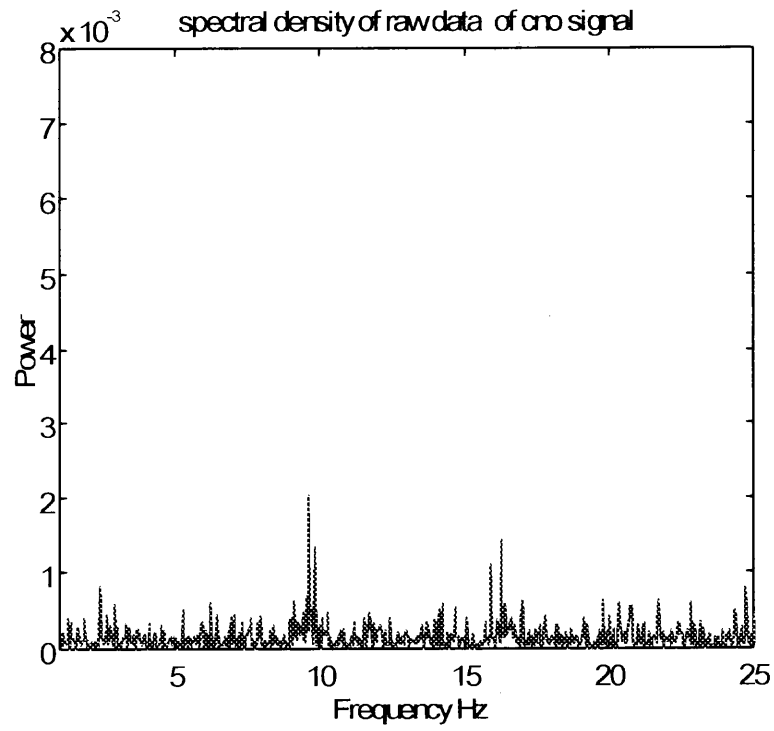
(a) eyes open
(b) eyes closed
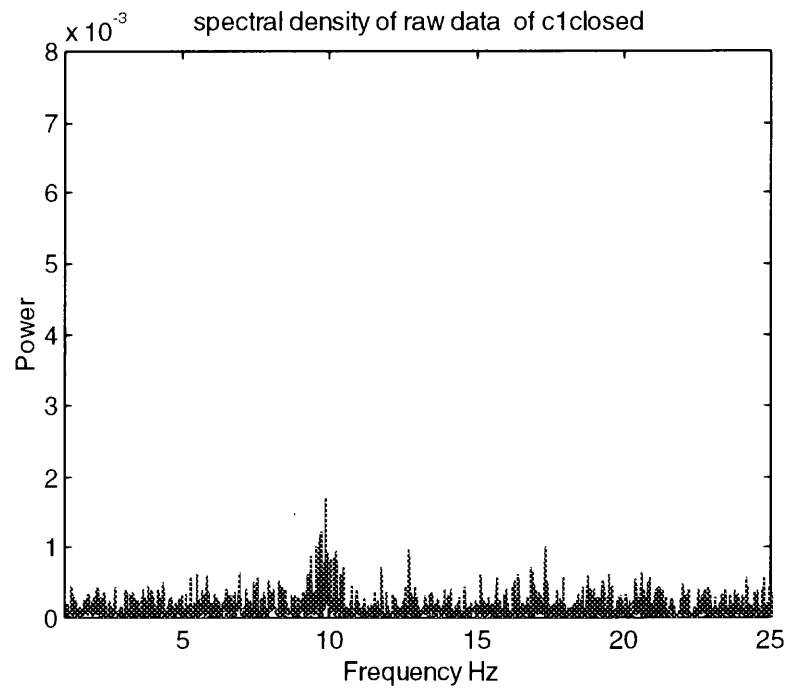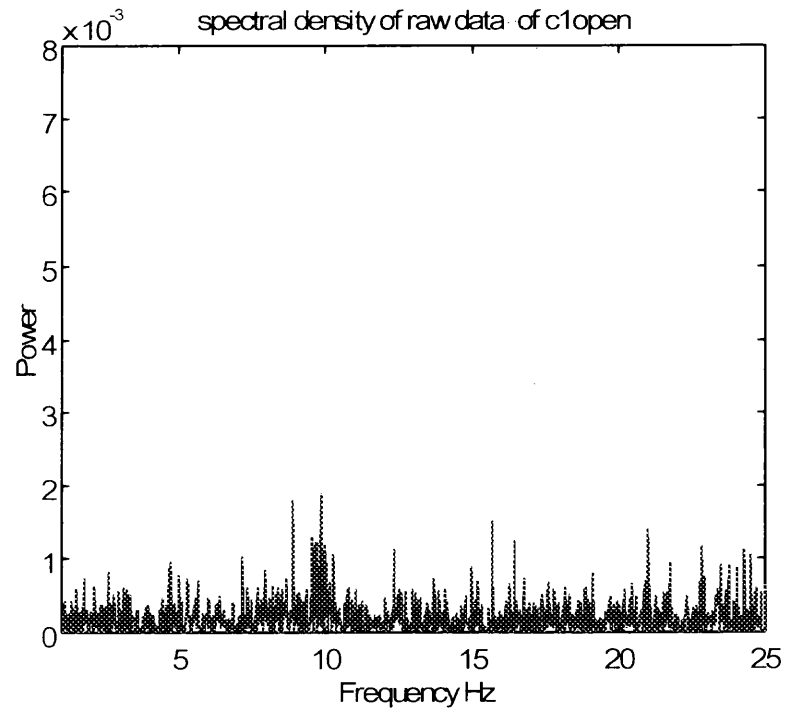
Figure 4.11 Frequency spectrum of Subject B through coil-based sensing.

(a) eyes open
(b) eyes closed

Figure 4.12 Frequency spectrum without a subject.

(a) eyes open
(b) eyes closed

CHAPTER 5

CONCLUSION

Drowsy driving can be assessed through the use of the Electroencephalogram, although recording via a non-obtrusive means still remains an unsolved issue. The sensitivity issues in recording Electroencephalogram signals pose limitations due to the recording methods followed. Electrode-based recordings reveal a distinction in states of awareness, which can be used to monitor drowsy driving. However, this method of recording is unacceptable in situations where obtrusiveness is an issue.

Coil-based recording offers a solution to non-obtrusive drowsy driver monitoring. By measuring brain signals from the occipital region of the scalp, the driver will not be subjected to any visual distractions or physical contact with the recording apparatus. An ideal setting would be to have a set of coils placed in the driver's headrest, where it can monitor his or her state of awareness. The recorded signals can then be used to alarm the driver of his or her condition. However, further research is needed to accomplish this goal. Instrumentation such as the Superconducting Quantum Interference Device (SQUID) is able to record such information, but at a high cost and lengthy recording procedure.

Differential amplifiers for biomedical purposes require high sensitivity as well as safety precautions. Utilizing the biquad filter configuration enables a high gain, sensitive design. Limitations do exist however in the number of stages used, as is the case in the small oscillation observed in the single-ended differential amplifier. The use of low-noise operational amplifiers enhanced circuit performance. With isolation being an issue in

direct-contact circuits, isolation amplifiers such as the AD202 offer simple, affordable solutions.

This study confirms that electroencephalogram recordings can play a role in detecting states of drowsy driving. However, it is clear that future research must focus on coil-based recording due to their distinct advantages. In solving problems such as recording and cost-effectiveness, portable coil-based drowsy driving detection systems can someday become a standard in all vehicles, leading to enhance safety. Further studies to improve differential coil configuration are to be made in the following areas:

- better magnetic coils with lower losses,

- amplifiers with lower noise figures,

- improved impedance matching between coils and amplifiers.

APPENDIX A

DATA ACQUISITION / ANALYSIS PROCEDURE

A.1 Labview data acquisition

- Load Labview 5.1
- Load "Continuously Acquire to Spreadsheet File.VI"
- Set device option to 1
- Set channel option to 0
- Set scan rate to 600 scans/sec.
- Set buffer size to 5000
- Set number of scans to write at a time to 300
- Select the "run" arrow at the top left corner of the screen.
- The program will ask you to enter a file name. Enter "filename".txt. This step creates the file which will download the incoming data.
- Press "enter" and the data collection will begin.
- Press the "STOP" button for the program to terminate.

A.2 Matlab Data Analysis

- Before we begin the analysis in Matlab, we must first edit the downloaded file. Labview-recorded spreadsheet files begin with the sampling rate as the first number of the file. Matlab spreadsheet files do not begin with the sampling rate. Therefore, when analyzing Labview spreadsheet files in Matlab, we must eliminate the first number. Otherwise, it is considered data by Matlab and incorrectly translates the results.
- Load Wordpad
- Open "Filename".txt
- Delete the first number of the file, which is the recorded sampling rate.
- Save file.
- Load Matlab 4.1
- Change the directory to c:\matlab\eeg
- Load the spreadsheet file into the matlab directory by typing:
    Load "filename".txt
- Load the sampling rate used by typing:
    Fs="sampling rate"
- Load the spreadsheet file into program's 'x' variable by typing:
    X="filename"
- the download data will begin to run. Press 'Ctrl' and 'C' at the same time to end.

- Type "spc_plt" to begin the frequency spectrum program.
- The program will ask you to enter a title for the plot. Enter title.
- Press enter and the graph is displayed.

APPENDIX B

COMPUTER PROGRAM

SPC_PLT is used to calculate and plot the power spectrum of the input signal.

```
f_str=input('enter graph title:','s');
fftsize=length(x);

    %put alternative fft method here
        x=x-mean(x);
        fftx=fft(x,fftsize);
        p=fftx.*conj(fftx)/fftsize;
        f=Fs*(0:(fftsize/2-1))/fftsize;
        clear fftx

    %plot(f(400:800),p(400:800)/max(p),'r');
    plot(f(10:2000),p(10:2000)/max(p)/40,'r');
    xlabel('Frequency Hz')
    ylabel('Power')
    title(sprintf('spectral density of raw data  of
%s',f_str));
                    axis([1 25 0 0.002]);
```

REFERENCES

[1]   R.R. Knipling, J.J. Wang, "Crashes Related to Drowsy Driving", November, 1994.

[2]   Institute for Traffic Safety, "Summary of New York State's Comprehensive
      Approach to Addressing Drowsy Driving", Albany, N.Y., 1998

[3]   K.P.Strohl, J. Blatt, F. Council, Kate Georges, J. Kiley, R. Kurrus, A.T. McCartt, S.
      L. Merrit, "Drowsy Driving And Automobile Crashes", NHTSA, November 2, 1999

[4]   R.W. Huey, J.L. Harpster, and N.D. Lerner, "In-Vehicle Crash Avoidance Warning
      Systems: Human Factors Considerations", NHTSA, Report No. Dot-Hs-808-531,
      February 1997.

[5]   F.S. Barickman and M.J. Goodman, "Micro Das: In-Vehicle Portable Data
      Acquisition System", *Transportation Research Record,* Paper No.99-0611, 1989.

[6]   D.M. Freud, R.R. Knipling, A.C. Landsburg, R.R. Simmons, and G.R. Thomas, "A
      Holistic Approach to Operator Alertness Reasearch", U.S. Department of
      Transportation, Paper No. 950636, January 1995.

[7]   R.M. Clarke, M.J. Goodman, M. Perel, and R.R. Knipling, "Driver Performance and
      IVHS Collision Avoidance System: A Search for Design-Revelent Measurement
      Protocols", NHTSA Report No. Dot-101-745, 1992.

[8]   L. Tijerina, M. Glecker, D. Stoltzfus, S. Johnson, "A Preliminary assessment of
      Algorithms for Drowsy and Inattentive Driver Detection on the Road",
      NHTSA Report No. Dot-HS-808, March 1999.

[9]   R.P. Hamlin and Northrop Grumman Corporation, "Three-In-One Vehicle
      Operating Sensor", National Research Council, Contract ITS-18, September 1995.

[10] R.D. Peters, E. Kloeppel, E. Alicandri, J. E. Fox, T.R. Thorne, H. C. Sing, and S.
      M. Balwinski, "Effects of Partial and Total Sleep Deprivation On Driving
      Performance", FHWA Report No.FHWA-RD-94-046, October, 1994.

[11] W.A. Leasure, Jr., A.L. Burgett, "Collision Avoidance Research Program: Strategic
      Plan and Status Update", NHTSA Paper No. 94-S3001, 1994.

[12] J.W. Clark, Jr., M.R. Neuman, W.H. Olson, R.A. Peura, F.P. Primiano, and M. P.
      Siedband, *Medical Instrumantation : Application and Design,* New York, John
      Wiley & Sons, 1998

[13] D.A. Newandee, "Measurements of the Electroencephalogram (EEG) Coherence.
      Atmospheric Noise, and Schumann Resonance in Group Meditation", Masters
      Thesis, New Jersey Institute of Technology, Newark NJ, 1996

[14] R.G. Brown , *Introduction to Random Signal Analysis and Kalman Filtering,* New York John Wiley & Sons, 1983